6-8-2011

Molecular dynamics predictions of thermal and mechanical properties of thermoset polymer EPON862/DETDA

Chunyu Li
Purdue University, lichunyu@purdue.edu

Alejandro Strachan
Birck Nanotechnology Center, Purdue University, strachan@purdue.edu

Polymer 52 (2011) 2920–2928

Contents lists available at ScienceDirect

Polymer

journal homepage: www.elsevier.com/locate/polymer

Molecular dynamics predictions of thermal and mechanical properties of thermoset polymer EPON862/DETDA

Chunyu Li, Alejandro Strachan*

School of Materials Engineering and Birck Nanotechnology Center, Purdue University, West Lafayette, IN 47907, USA

ARTICLE INFO

Article history:
Received 5 April 2011
Accepted 16 April 2011
Available online 23 April 2011

Keywords:
Thermoset
Molecular dynamics
Glass transition
Conversion degree

ABSTRACT

We use molecular dynamics (MD) to perform an extensive characterization of the thermo-mechanical response of a thermoset polymer composed of epoxy EPON862 and curing agent DETDA. Our simulations, with no adjustable parameters, show that atomistic simulation can capture non-trivial behavior of amorphous thermosets including the role of polymerization degree, thermal history, strain rate and temperature on the glass transition temperature (T_g) and mechanical response (including ultimate properties) and lead to predictions in quantitative agreement with experiments. We find a significant increase in T_g, Young's modulus and yield stress with degree of polymerization while yield strain is significantly less sensitive to it. For structures cured beyond the gel point (percolation of a 3D network) conversion degree and temperature affect yield stress in a similar way with yield stress linearly dependent on $T-T_g$; however, we find non-linear and non-universal relationship below the gel point. Our results show that a relative small variation in polymerization degree (~5%) can explain the spread in experimental measurements of T_g and elastic constants available in the literature.

1. Introduction

Thermoset polymers are the matrix of choice for fiber-reinforced composites used in a wide variety of applications including aerospace due to their high stiffness, strength as well as creep and thermal resistance as compared to thermoplastic polymers. These properties depend not only on their chemistry or composition but also on molecular structure and, consequently, polymerization (or conversion) degree as well as thermal history and testing conditions. In this paper we use molecular dynamics (MD) to characterize how conversion degree, annealing rate and temperature affect the thermo-mechanical response (including glass transition temperature, elastic properties and ultimate mechanical response) of EPON862 with curing agent DETDA.

Curing time and temperature play an important role in determining the network topology as well as the degree of conversion and there have been extensive experimental studies to characterize the effect of conversion degree on material properties of thermoset polymers. Among the properties studied, glass transition temperature is the most extensively characterized one. The dependence of glass transition temperature on conversion degree has been characterized, among others, for DGEBA/TMAB [1], epoxy/novolac, and dicyanate ester/polycyanurate [2], EPON828/MHHPA [3] Bisphenol-S/4,4′DDM [4] and toughened epoxy resin [5]. A general trend of all these experimental studies is that T_g increases with increasing conversion in a non-linear fashion with an increasing dependency for higher conversion degree. There have also been a few efforts involving atomistic simulations on the effect of conversion degree on T_g [6,7]; while a detailed characterization is still lacking, these have confirmed the general trends observed experimentally.

The role of conversion degree on mechanical properties of thermoset polymers remains poorly understood and different trends have been reported. Based on their comparison of elastic moduli of 14 epoxide-amine systems, Morel et al. [8] concluded that the effects of crosslinking density and glass transition temperature on the elastic properties of the polymers in the glassy state are insignificant. However, the studies of Ellis et al. [9] found a linear decrease of the room temperature Young's modulus (below T_g) with increasing T_g for BADGE/DDM epoxy resin. More recently, Marks and Snelgrove [10] also reported that a uniform trend of decreasing tensile modulus with increasing conversion for various amine-cured epoxy thermosets including DER332/EDA, DER332/DETA, and DER332/4,4′DDS.

Beyond elastic properties, the ultimate mechanical properties of thermoset polymers are critical for most applications. Generally, it is believed that a high conversion tends to increase yield stress but a decrease in fracture toughness as the material becomes more brittle [11]. However, the studies of Marks and Snelgrove [10] indicated that the trends of fracture toughness of amine-cured

* Corresponding author.
E-mail address: strachan@purdue.edu (A. Strachan).

0032-3861/$ – see front matter © 2011 Elsevier Ltd. All rights reserved.
doi:10.1016/j.polymer.2011.04.041

epoxy thermosets depend strongly on the structure of the curing agent and the degree of cure. The fracture toughness of thermosets often exhibits a maximum for conversion degrees between 65% and 95%, depending on the rigidity of curing agent. A molecular-level understanding of these trends is currently lacking, yet this knowledge would be highly desirable for the design of new thermoset polymers with desired properties and to understand current systems. Non-equilibrium MD is a powerful tool to uncover the molecular processes that govern yield and provide insight into the role of chemistry and molecular structure. A limitation of this technique is the short timescales achievable that lead to fast deformation rates; these effects need to be accounted when analyzing MD results. Prior MD simulations have provided insight into yield criteria of amorphous polymers [12] and post-yield behavior [13]; furthermore, progress is being made in understanding the relationship between macroscopic yield and atomic process [14]. Despite this progress, many questions remain unanswered especially for thermoset polymers and the relationship between molecular structure and yield and post-yield behavior.

In this paper we build atomic structures of EPN862/DETDA thermoset polymers using a procedure that combines MD simulations with distance-based chemistry models [15] similar to prior thermoset building methods [16] and characterize the thermo-mechanical response (including ultimate mechanical properties) of the resulting structures. In particular we focus on the effect of conversion degree, thermal history (cooling rate), temperature and strain rate on the thermal and mechanical properties.

2. EPON862/DETDA systems and interatomic potentials

The initial model system for our simulations consists of 256 monomers of EPON862 and 128 monomers of DETDA. The molecular structures of EPON862 and DETDA are shown in Fig. 1. As was done in previous studies [10,16], we start with the "activated" EPON862 shown in Fig. 1(b). The initial number of atoms in the model system is 16,000.

The DREIDING force field [17] with Buckingham functions (exponential repulsion and power 6 attraction) for van der Waals interactions is employed in all our simulations using the open source MD code LAMMPS [18]. The atomic charges are obtained from self-consistent calculations using the electronegativity equalization method as described in Ref. [15]. This approach to describe atomic interactions, that is generally applicable to any polymer and many composites, has been shown to provide an accurate representation of the thermo-mechanical properties of EPON862/DETDA [15] and EPON825/3,3′DDS [19] and other soft materials, see for example Ref. [20]. The importance of charge equilibration and electrostatic energy is quantified in the Supplementary material [21].

The method used to create the atomistic structure of the polymer is described in detail in Ref. [15] and we provide a brief description here for completeness. The procedure consists of two main stages (see flowchart shown in Fig. 2):

i) A mixture of the epoxy and curing agent with the desired stoichiometry is packed into a simulation cell with 3D periodic boundary conditions at low density (0.5 g/cm^3). The system is initially energy-minimized using the conjugate gradients method and then equilibrated using an isothermal and isochoric (NVT ensemble) MD simulation for 50 ps at 600 K followed by an isothermal, isobaric (NPT) MD simulation for 400 ps at atmospheric pressure.

ii) During the curing stage, chemical reactions are simulated in a stepwise manner using a distance-based criterion. Bonds are created between reactive atoms within a cutoff distance taken as four times the equilibrium NC bond length (1.41 Å). New bonds are turned on slowly using a 50 ps-long multi-step relaxation procedure to avoid large atomic forces. After the new bonds are fully relaxed an NPT simulation for an additional 50 ps is performed before the new set of bond creations is attempted. This procedure is continued until the total simulation time or conversion limit are achieved. The MD simulations during polymerization are carried out at 600 K to increase molecular mobility and reduce strain during the formation of the 3D thermoset network.

Structures with conversion degrees from 0% to 86% are selected from this procedure and their thermo-mechanical response characterized. The degree of conversion is defined as the ratio between the number of bonds created and the maximum possible bonds (four times the number of DETDA molecules).

3. Role of curing degree on glass transition temperature

After the polymerization and crosslinking procedure described above produces equilibrated structures at 600 K with various

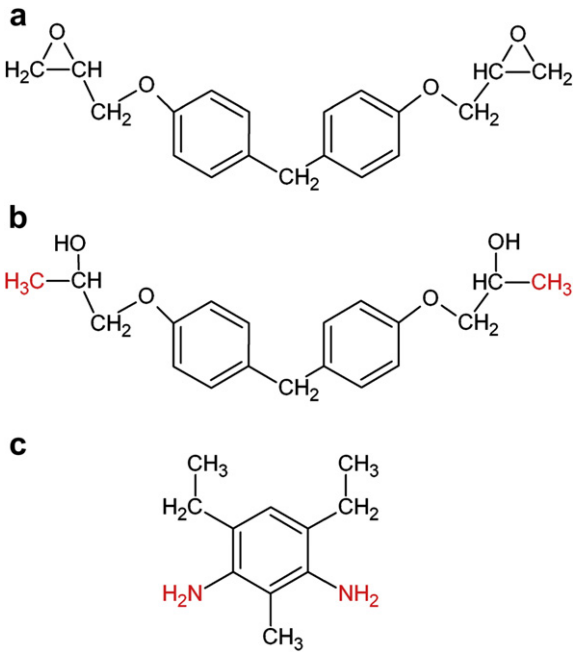

Fig. 1. Molecular structures of (a) EPON862, (b) activated EPON862 and (c) DETDA.

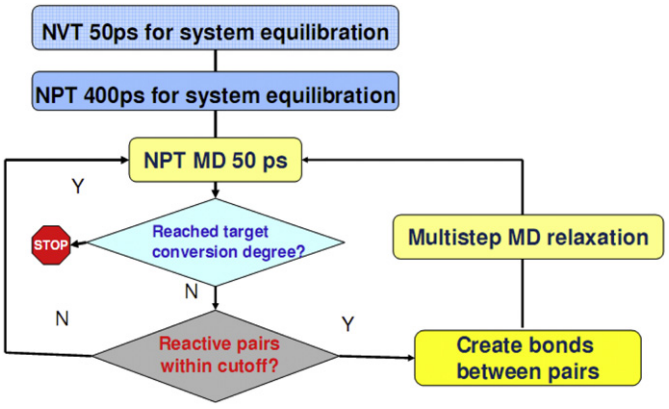

Fig. 2. Flowchart of curing procedure.

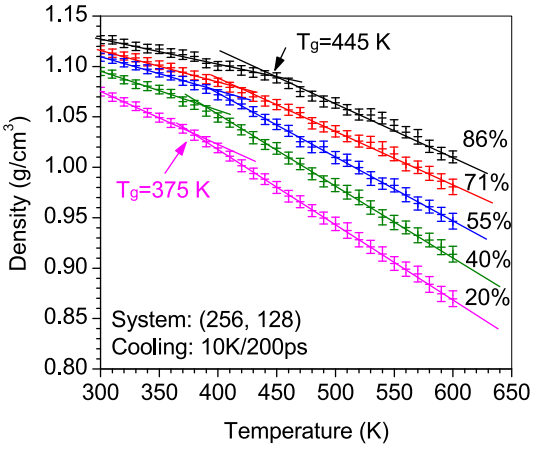

Fig. 3. Density as a function of temperature.

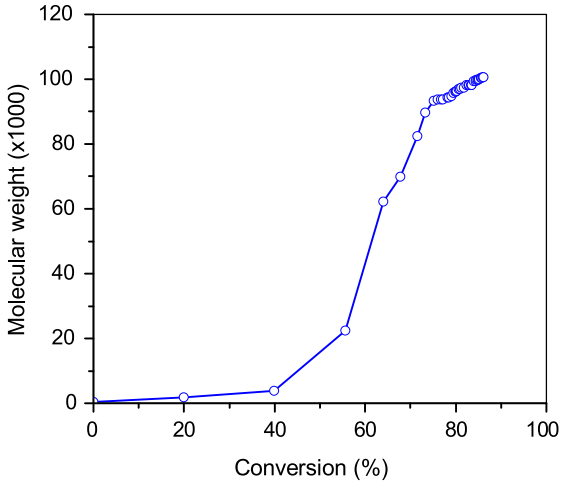

Fig. 5. Molecular weight of largest molecule as a function of conversion degree.

degrees of polymerization, we cool them down to room temperature using NPT MD simulations; from these simulations we characterize the glass transition temperature. In our simulations, cooling is performed in steps of 10 K and at each temperature we perform a 200 ps-long simulation at atmospheric pressure. Fig. 3 shows density-temperature plots for our epoxies with various degrees of conversion; we predict an increase in density and T_g (marked by a change in slope of the density-temperature curves) as the conversion degree increases. This information is displayed in Fig. 4 where T_g is plotted as a function of conversion degree. T_g and associated error estimates are obtained from the density-temperature data, Fig. 3, using segmented regression ($R^2 > 0.9997$ with p*p* value <0.0001 for F_test). Our simulations show that T_g increases by about 80 K when the conversion degree goes from 0% to 86%. The dependency of T_g with curing degree becomes more pronounced as the curing proceeds. Interestingly, a significant increase in the slope of T_g vs. conversion degree occurs at around 60% conversion. This corresponds to the conversion degree where we observe a significant slowdown in the rate of chemical reactions during polymerization [15] and where the molecular weight of the largest molecule increases significantly as shown in Fig. 5. The steep increase in the mass of the largest molecule containing the majority of the mass in the system indicates the percolation of a 3D network and the gel point. These results are in agreement with prior simulations [16].

The reported experimental T_g values for EPON862/DETDA are 413 K [22] and 417–432 K [23] and in order to compare these values

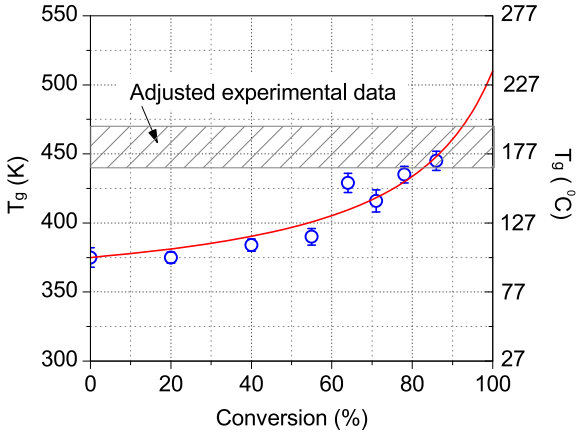

Fig. 4. T_g as a function of conversion.

with our MD data the role of cooling rate should be taken into account since T_g is a kinetic quantity. Higher rates of heating and cooling increase T_g and this effect can be quantified via the classic William–Landel–Ferry (WLF) equation [24,25], that describes the relation between relaxation time and temperature measured from a reference value and was obtained empirically from extensive experimental measurements on various glass formers from polymers to organic liquids. The WLF equation leads to an increase in T_g of 3 K per order of magnitude increase in cooling or heating rate [25]. Thus, the T_g predicted from our MD (with a rate of 5×10^{10} K/s) should be expected to be about 30 K higher than the experimental value, i.e. ~440–470 K, which is shown in Fig. 4 as adjusted experimental data. Our predictions for high conversion degrees (over approximately 85%) are in agreement with available experimental data and while the conversion degree in those experiments was not reported but typical values are believed to be around 90%. Our simulations indicate that a likely contributing factor for the range of experimental T_g values reported in the literature is the variation in conversion degree among the various tests.

DiBenedetto's equation has been shown to describe the relation between T_g and conversion degree from experiments [26,27], it can be written as:

$$\frac{T_g - T_g^0}{T_g^\infty - T_g^0} = \frac{\lambda\xi}{1-(1-\lambda)\xi} \tag{1}$$

where λ is an adjustable parameter that describes non-linearity in the T_g-conversion curve, ξ stands for the conversion degree, T_g is the glass transition temperature at conversion degree ξ and T_g^0, T_g^∞ are the glass transition temperatures for conversion degrees of 0 and 1, respectively. In order to describe the MD data, we use a least squares method to obtain λ and T_g^∞ from our MD T_g values. The resulting curve, shown as a solid line in Fig. 4, corresponds to $T_g^\infty = 510$ K and λ=0.19. We are unaware of experimental characterization of the dependency of T_g on conversion degree for EPON862/DETDA, our predicted value for λ falls in the range of 0.16–0.6 reported in the literature [2]. Using DiBenedetto's equation our T_g predictions can be extrapolated to higher conversion degrees that are difficult to achieve with atomistic simulations.

4. Mechanical response

We characterize the mechanical response of the EPON862/DETDA samples via non-equilibrium MD simulations of uniaxial

deformation. These simulations are carried out by continuously (i.e. at each MD step) increasing the length of the simulation cell along one of its cubic directions and maintaining atmospheric pressure in the transverse directions using a barostat. We assume the material to be isotropic and maintain the simulation cell lengths in the directions transverse to the tensile axis equal to each other at all times. Uniaxial deformations are carried out along all three Cartesian directions from which average stress–strain curves are obtained. Samples are deformed up to a longitudinal strain of 50% with two strain rates: 5×10^8 s^{-1} and 5×10^9 s^{-1}. While much higher than in experiments, these rates are typical of non-equilibrium MD simulations [12–14].

4.1. Role of conversion degree

Fig. 6(a) shows the longitudinal engineering stress versus engineering strain curves for systems with various conversion degrees at a strain rate of 5×10^8 s^{-1}. We obtain the Young's moduli of our model epoxy by fitting the MD data to a linear function up to strains of 2% and 4%. The two limits provide a measure of the uncertainty in the predictions due to the standard fluctuations present in MD simulations and are chosen due to the weak non-linearities in the stress–strain relationship up to 5% strain (non-linearities in the stress–strain curves are analyzed in the Supplementary material [21]). The dependence of Young's modulus on conversion degree is shown in Fig. 6(b). Our simulations show a significant stiffening of EPON862/DETDA from approximately 1 GPa to about 3 GPa as the 3D network forms. The moduli for larger conversions compare well with existing experimental data; for example, Sun et al. [22] and Zhou et al. [28] reported a Young's modulus of 2.76 GPa and 2.46 GPa, respectively, for neat epoxy EPON862/DETDA, while Tack [29] obtained an average Young's modulus of 2.5 GPa for EPON862/DETDA with a standard deviation of ±0.6 GPa. A stress–strain curve from a tensile experiment on EPON862/DETDA [22] is also shown in Fig. 6(a) for comparison (circles). As expected for tensile testing at room temperature brittle fracture is observed in the experiments while the small periodic samples used in the MD simulations are unable to localize strain and exhibit significant inelastic behavior. Fig. 6(c) shows the transverse strain as a function of the longitudinal strain from our MD simulations at a strain rate of 5×10^8 s^{-1}. The initial slope of these curves represents the predicted Poisson's ratio and we compute it by fitting linear functions to the MD data up to strains of 2% and 4%. We find that the conversion degree has a considerable effect on Poisson's ratio, see Fig. 6(d). Poisson's ratio decreases with conversion degree from slightly less than 0.5 for the unreacted mixture of EPON962 and DETDA. For conversion degrees higher than 60% the predicted values have a mean of 0.31 and a standard deviation of 0.11. This average value for high conversion degrees is in reasonable agreement with the available experimental data 0.353 [29]. Such regime, of interest in most applications, corresponds to the presence of a percolating network, see Fig. 5, and we speculate that the large fluctuations in the MD data are associated with changes in the network structure. Note that the increase in room temperature Poisson ratio toward 0.5 (the value of a liquid sample) with decreasing conversion degree has two origins, one being the change in the network structure of the polymer; secondly the testing temperature becomes closer to T_g.

From Fig. 6(a) it is clear that the yield stress increases with increasing conversion degree. In order to quantify this effect we must overcome the fact that the large fluctuations stemming from

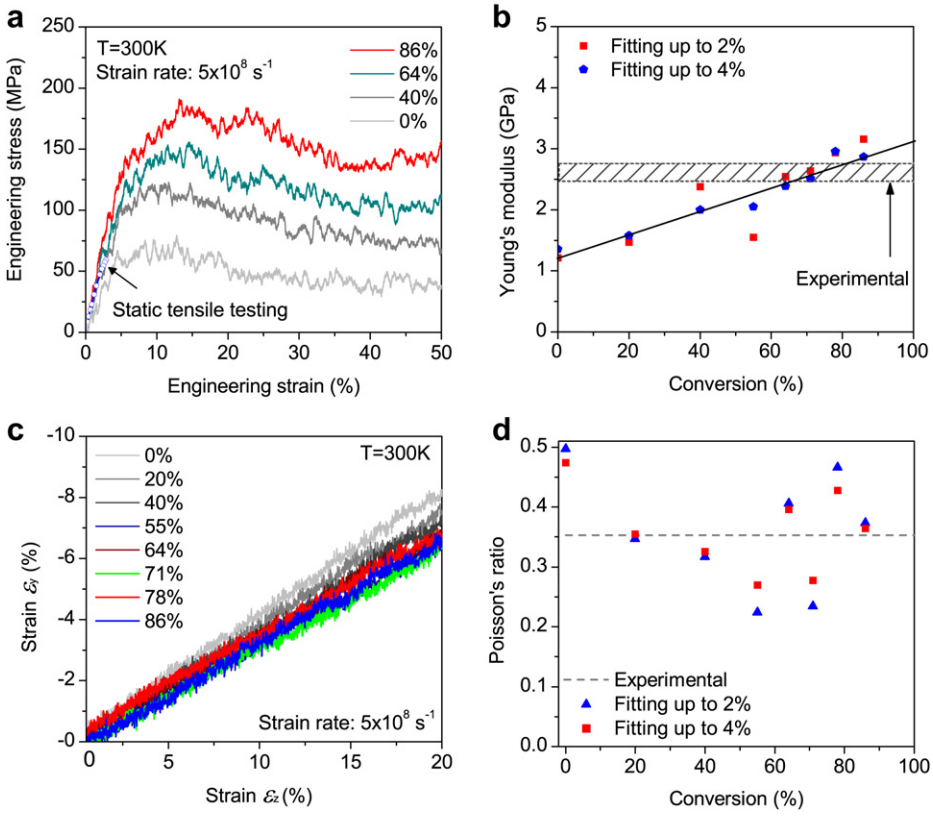

Fig. 6. (a) Longitudinal stress as a function of longitudinal strain for samples with various degrees of conversion; (b) Predicted Young's modulus as a function of conversion degree (experimental values are from Refs. [22,28,29], the black line shows the trend of the simulation data); (c) Lateral strain as a function of longitudinal strain for samples with various conversion degrees; (d) Poisson's ratio as a function of conversion degree (experimental value from Ref. [29]).

the relatively small simulation cells make it hard to accurately identify the yield point. Thus, we fit quadratic functions to the stress–strain data around the maximum of the MD data and associate the yield point with the maximum of the fit. Table 1 shows the fitting range used for each conversion degree and the resulting yield stress and strain. Error estimates for the yield stress and strain are obtained from the standard errors in the fitted value of the quadratic function. Fig. 7(a) and (b) show the yield stress and strain as a function of conversion degree, respectively. The resulting yield stress increases by a factor of over two as the unreacted mixture is converted to 86%. This relative increase is similar to that associated with Young's moduli which is consistent with the yield strain being relative insensitive to conversion degree, Fig. 7(b). This is an important result that indicates that yield criteria based on strain instead of stress may be better suited for this class of polymers.

There are no reports of strength of EPON862/DETDA for strain rates comparable to the ones accessible to MD simulations and, since a strong sensitivity of strength with strain rate is firmly established [30], we expect the available experimental values to be significantly smaller than our MD predictions. Besides the effect of strain rate, differences in ultimate mechanical properties between MD simulations and experiments can originate in the fact that the small system size in the simulations precludes strain localization and brittle failure. Sun et al. [22] reported a 64 MPa tensile strength for neat epoxy EPON862/DETDA based on their tensile testing using an MTS servo-hydraulic test machine, on the other hand Zhou et al. [28] obtained a 93.5 MPa tensile strength for neat epoxy EPON862/DETDA based on their three-point flexural tests; these results are shown in Fig. 7(a).

4.2. Role of strain rate and cooling rate

The mechanical response of the amorphous polymers is known to depend on both the rate of deformation and the thermal history of the sample (cooling rate used to generate the $T = 300$ K structure in our case) and in this Section we explore these effects on EPON862/DETDA.

Fig. 8 shows stress–strain curves for systems with a conversion degree of 86% at two different strain rates: 5×10^8 s^{-1} and an order of magnitude faster, 5×10^9 s^{-1}. Our simulations show that the Young's modulus is insensitive to strain rate; on the other hand, yielding is strongly affected by the rate of deformation. Yield stress increases with strain rate as the polymer is less able to relax in response to the deformation. The order of magnitude increase in strain rate leads to an increase in yield stress of approximately 40 MPa; this trend was observed in Hopkinson bar experiments on various thermosetting polymers [30]. Despite the fluctuations inherent in small-scale simulations, our results indicate that yield strain is less sensitive to strain rate than yield stress; this is also consistent with experiments [30]. For both strain rates we observe slight softening following yield and hardening for strains larger that ~35%.

Table 1
Fitting stress–strain curves around maximum.

Conversion (%)	Strain fitting range (%)		Yield stress (MPa)	Yield strain (%)
86.0	11	18	182 ± 24	14.6 ± 0.6
78.0	8.5	17	167 ± 11	12.8 ± 1.5
71.0	8.5	17	164 ± 15	12.7 ± 0.9
64.0	8.5	17	146 ± 10	13.6 ± 1.3
55.0	8.0	15	136 ± 13	11.4 ± 0.7
40.0	7	14	117 ± 10	10.3 ± 0.8
20.0	6.5	13.5	91 ± 10	11.1 ± 1.2
0.0	6.0	14.0	67 ± 9	11.5 ± 2.9

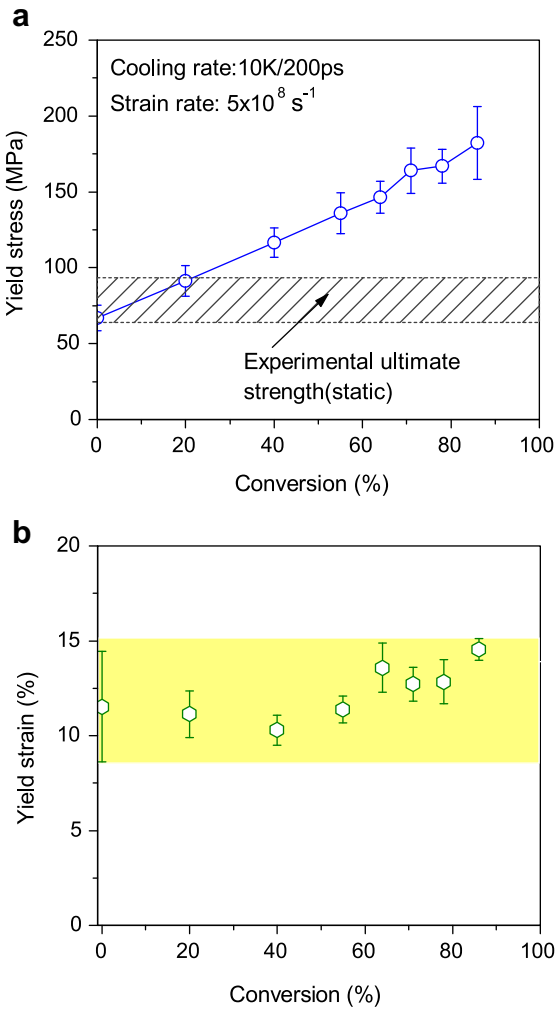

Fig. 7. (a) Predicted yield stress as a function of conversion degree (experimental data from Refs. [22,28]); (b) Strain at yield peak as a function of conversion degree.

Fig. 9(a) and (b) show how the stress–strain curves depend on the rate used to cool the samples down from 600 K to 300 K. Fig. 9(a) shows results for a strain rate of 5×10^8 s^{-1} and Fig. 9(b) for 5×10^9 s^{-1}. In both cases we find that the slower cooling rate leads

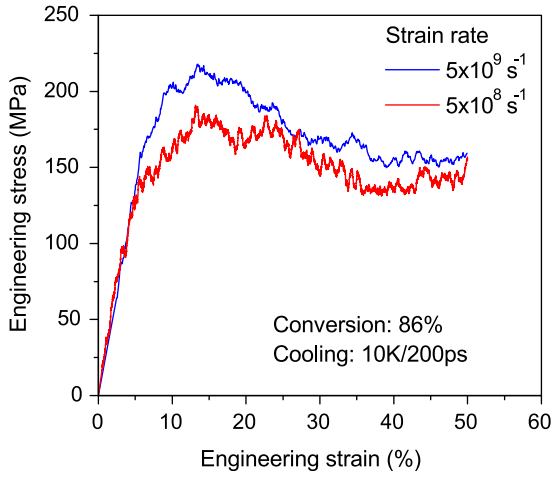

Fig. 8. Stress–strain curves for EPON862/DETDA polymer with 86% conversion for two different strain rates.

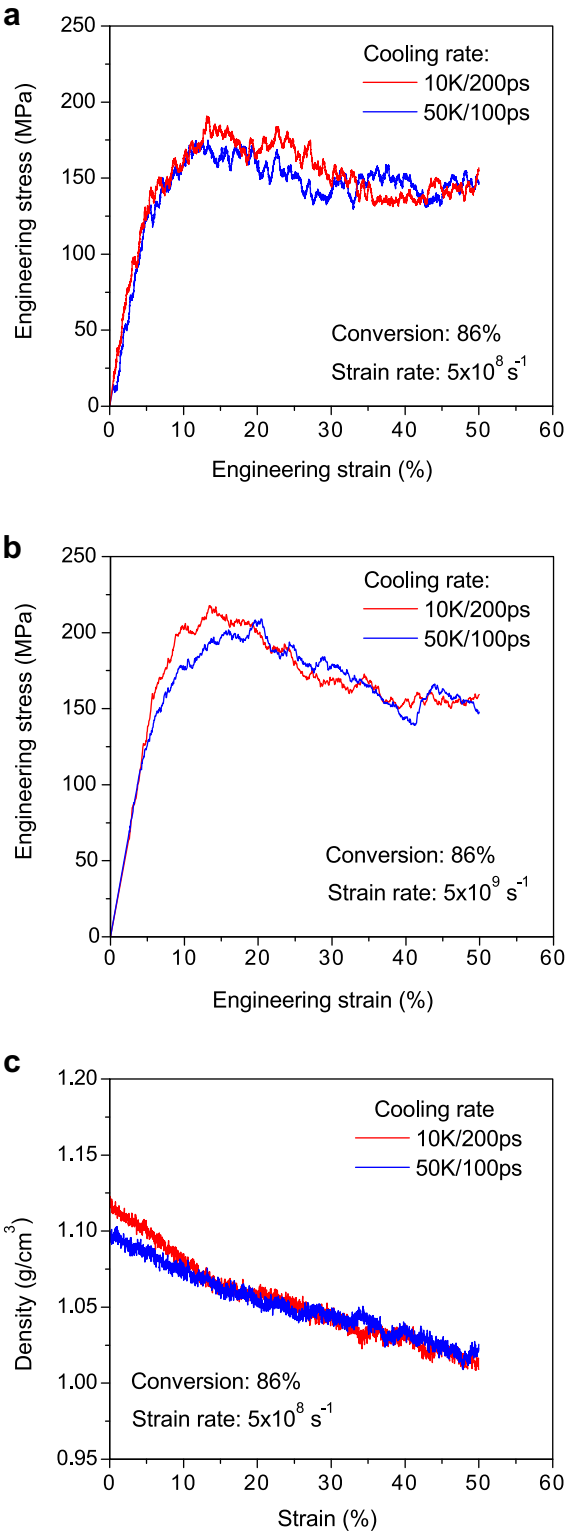

Fig. 9. Role of cooling rate on ultimate mechanical response. Stress–strain curves of samples that have undergone different cooling rates (10 K/200 ps, blue, and 50 K/100 ps, red) for a strain rate of (a) 5×10^8 s^{-1} and (b) 5×10^9 s^{-1}; (c) Density as a function of strain for samples with different cooling rates for a strain rate of 5×10^8 s^{-1}. (For interpretation of the references to colour in this figure legend, the reader is referred to the web version of this article).

to a higher yield stress but, after yield, the yield stress becomes essentially independent of cooling rate. Slower cooling rates lead to better relaxation of the thermoset structures and, consequently, an increase in the yield stress as previously observed in glassy thermoplastic polymers [31]. The temporal evolution of the polymer densities during deformation sheds light into the physics that govern the effects of thermal history, see Fig. 9(c). Prior to deformation the sample cooled down at a lower rate exhibits a higher density than the fast-cooled sample, this higher density denotes better relaxation and lead to a higher yield stress during deformation. However, once inelastic deformation begins the sample's thermal history is *erased* (at least from the point of view of stress) and both yield stress and density [Fig. 9(c)] of the two samples with different thermal histories collapse into a single curve.

4.3. Role of temperature

Fig. 10 shows the engineering stress-engineering strain curves for a system with 86% conversion under different temperatures. As expected both the Young's modulus and yield stress decrease with increasing temperature; we predict a Young's modulus decrease of approximately 1 GPa per 100 K temperature increase, as shown in Fig. 10(b), and a yield stress decrease of approximately 60 MPa for a temperature increase of 100 K, as shown in Fig. 10(a).

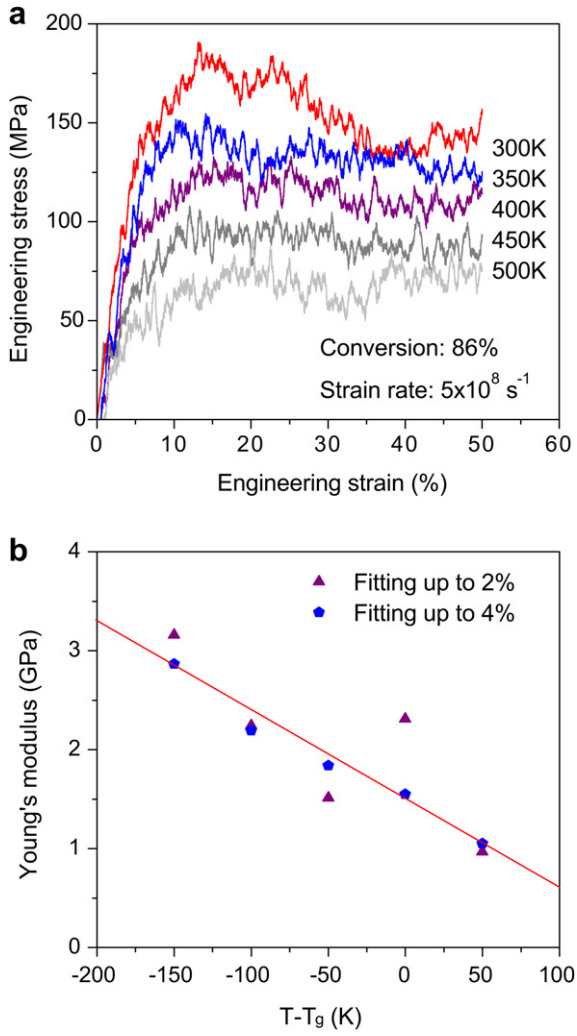

Fig. 10. Effect of temperature on stress–strain relationship for a polymer with 86% conversion. (a) Stress–strain curves at different temperatures; (b) Young's modulus versus temperature.

5. Discussions

5.1. Role of conversion and temperature on yield stress

Two factors affect the increase of room temperature yield stress with conversion degree shown in Figs. 6(a) and 7(a). First, the increase in molecular weight and network connectivity. Second, the increase in T_g with conversion degree leads to a reduction in testing temperature when measured from T_g ($T-T_g$). To help quantify these effects Fig. 11 shows the room temperature yield stress as a function of $T-T_g$ for systems of varying conversion degrees together with the yield stress of a system with 86% conversion at $T = 300$, 350, 400 K also as a function of $T-T_g$. For low conversion degrees there is a rapid increase in yield stress with decreasing $T-T_g$ but for samples with over 60% conversion the increase rate in yield stress is reduced. This change in behavior coincides with the formation of a percolating polymer network (gel point) and indicates that for highly crosslinked thermosets increasing the degree of curing increases their thermal stability more than their ultimate mechanical properties as compared with conversions degrees below the gel point. A comparison of the room temperature yield stress for various conversions with the temperature dependent yield stress as functions of $T-T_g$ shows that as the conversion is increased over the gel point the strengthening originates from an increase in T_g. For conversion degrees over the gel point our results show the same physics as what is observed in thermosets with varying molecular weight between crosslinks; see for example Refs. [32,33]. Lesser and collaborators used various crosslinking molecules and chain extenders to control the molecular weight between crosslinks in epoxy thermosets and showed the yield stress to be a function only of $T-T_g$ for materials with similar backbone stiffness [32]. Our simulations also predict a linear relationship between yield stress and ($T-T_g$) for conversions over the gel point, also in agreement with experimental data, see for example Ref. [11]. Due to the ability to control conversion degree exactly in the simulations we are able to characterize the roles of molecular structure and temperature on the same polymer as a function of conversion (a very difficult task to accomplish experimentally). Our simulations show that for high conversion degrees, the effect of increasing conversion on the yield stress can be explained by the increase in T_g, while below the gel point the yield stress deviates from this behavior.

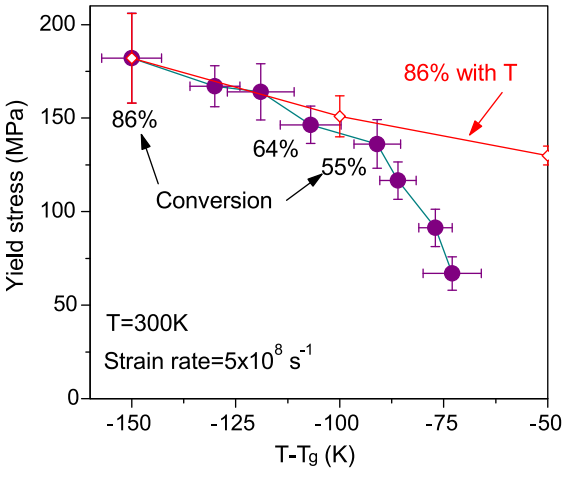

Fig. 11. Room temperature yield stress for polymers with different conversion degrees (full circles) and yield stress of the system with 86% conversion at various temperatures [from Fig. 10(a)] as a function of $T-T_g$.

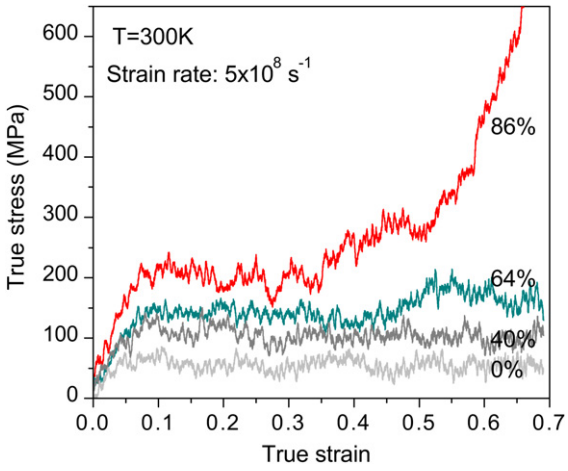

Fig. 12. True stress-true strain relationship for different conversions.

5.2. Trends in yield and post-yield behavior

In order to discuss post-yield phenomena we plot true stress-true strain curves for various conversion degrees at $T = 300$ K in Fig. 12 and for various temperatures for a sample with 86% conversion in Fig. 13. Each curve shown in Figs. 12 and 13 is the result of a single MD run as opposed to averages over deformations along the x, y and z axes as is the case for all prior deformation results. Fig. 12 shows softening immediately following yield for all cases. While this softening continues to very large strains for samples with 0% and 40% conversion, the 64% sample shows slight hardening for strains over 0.4. For even higher conversion degrees, when a 3D network is formed, the hardening begins at lower strains and is significantly more pronounced.

Increasing the testing temperature not only decreases the yield stress, as described above, but also the post-yield softening, Fig. 13. Actually we do not observe softening for temperatures of 400 K and higher; as the timescales associated with structural relaxation decrease with increasing temperature the polymer is able to adjust to the deformation more readily, reducing the stress overshoot at the yield point and post-yield softening. Larger-scale simulations, with smaller fluctuations, will enable a quantitative characterization of softening and hardening moduli for various conditions but we expect the general trends described here to remain valid.

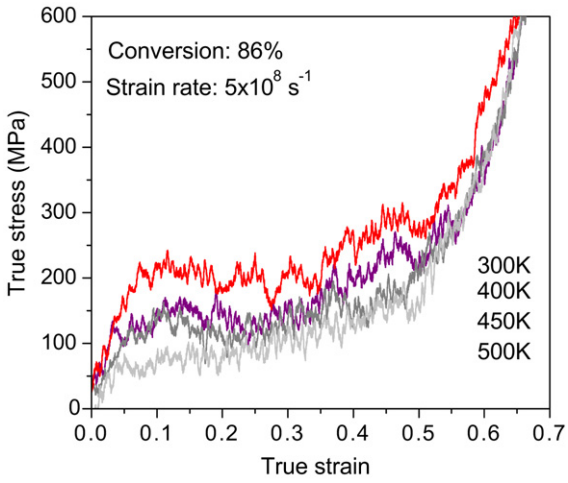

Fig. 13. True stress-true strain relationship at different temperatures.

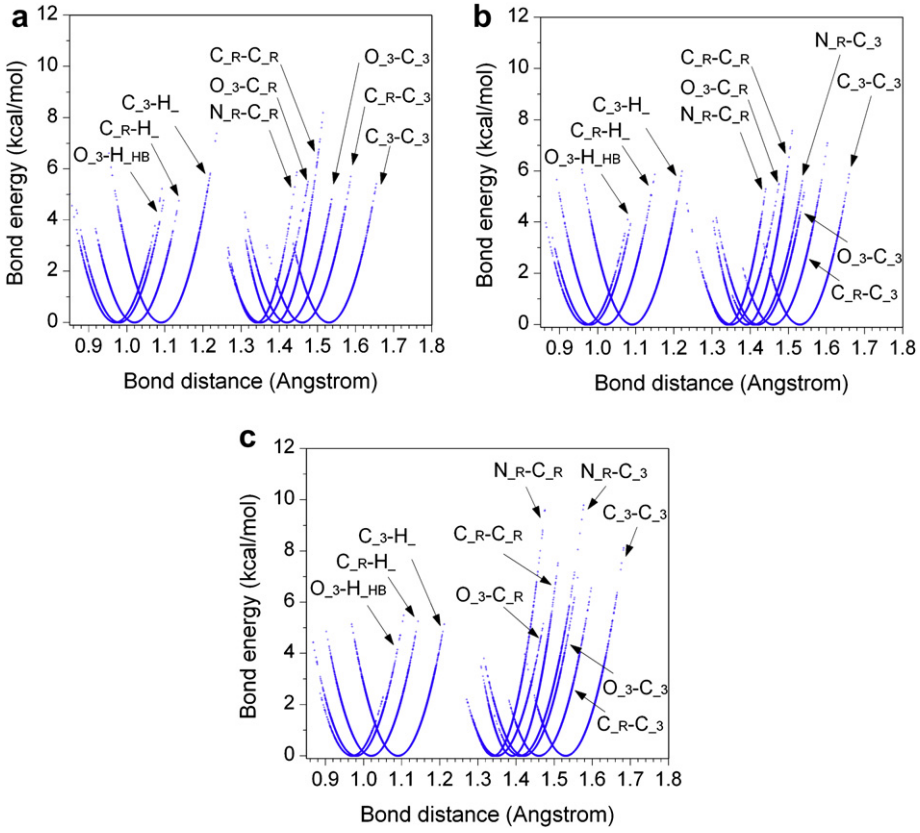

Fig. 14. Energy-distance curves for all covalent bonds in samples deformed at 300 K to 100% tensile strain for (a) 0% conversion, (b) 64% conversion, and (c) 86% conversion.

Figure S-1 in the Supplementary material [21] compares stress–strain data for two different sizes for a high conversion degree system.

5.2.1. Bond stretch analysis at large strains

Our MD approach to characterize the thermo-mechanical properties of the polymer systems is non-reactive, i.e. we do not allow for chemical bond breaking or the formation of new bonds. We now analyze whether this assumption is justified for the large deformation levels investigated. Fig. 14 plots the bond energy as a function of bond distance for all chemical bonds in the system for an atomic snapshot at 100% engineering strain for samples with 0% conversion, Fig. 14(a), 64% conversion, Fig. 14(b) and 86% conversion, Fig. 14(c). Interestingly, the analysis of bond distributions indicates that even for such a large amount of strain bond energies (not larger than 10 kcal/mol) remain significantly lower than what is needed for bond breaking (the dissociation energy for a C–C bond in ethane is 98 kcal/mol). The relatively small bond energies justify the use of harmonic bonds in these simulations. Thus, local strains larger than 100% would be required for chemical bond scission in this class of epoxies. These levels of strain are unimaginable in macroscopic samples as a whole where brittle failure occurs at much lower average strains. However, large strains are expected in regions of localized deformation like crazes or shear bands. Strain localization cannot occur in the MD simulation cells to the same degree due to the small size of the MD samples.

7. Conclusions

In this paper we used MD simulations to provide a rather thorough characterization of the thermo-mechanical response of the thermoset polymer composed of the epoxy EPON862 and curing agent DETDA for various degrees of polymerization, thermal history, strain rate and temperature. MD simulations enable, without any tunable parameters, the description of the molecular structure and thermo-mechanical properties of amorphous thermosets, naturally capturing non-trivial behavior including: the role of thermal history, strain rate and temperature on mechanical properties including yielding and post-yield behavior.

Our simulations characterize how glass transition temperature (T_g) and mechanical properties depend on degree of polymerization. We find T_g, stiffness and yield stress depend strongly on conversion degree even near full conversion. While such characterization remains experimentally challenging due to difficulties in monitoring and controlling the degree of curing, the sensitivity of thermo-mechanical properties to conversion degree predicted by our simulations underscores the importance of taking degree of cure into account in the analysis and interpretation of experimental data or theoretical predictions as well as in the design of processing conditions.

Our MD predictions, using the general purpose Dreiding force field with Buckingham van der Waals interactions, are in good agreement with available experimental results. Thus, the results could be used to inform continuum viscoelastic constitutive models, see for example Ref. [34], capable of predicting the behavior of macroscopic samples including their use in polymer matrix composites of interest for structural applications. We foresee that once the connections between chemistry and atomic interactions and the macroscopic world are established and validated, predictive computational tools will facilitate the design and certification of new thermoset polymers reducing the need for time-consuming and expensive experiments.

Acknowledgments

This work was supported by a grant with The Boeing Company and the US National Science Foundation (NSF) under contract CMMI- 0826356. Useful discussions with G. Medvedev, J. A. Caruthers, R. B. Pipes, S. Christensen and J. Gosse are gratefully acknowledged.

Appendix. Supplementary data

Supplementary data associated with this article can be found, in the online version, at doi:10.1016/j.polymer.2011.04.041.

References

[1] Wang XR, Gillham JK. J Appl Polym Sci 1991;43:2267–77.
[2] Venditti RA, Gillham JK. J Appl Polym Sci 1997;64:3–14.
[3] Boey FYC, Qiang W. J Appl Polym Sci 2000;78:511–6.
[4] Gao JG, Li YF, Zhao M, Liu GD. J Appl Polym Sci 2000;78:794–9.
[5] Simon SL, McKenna GB, Sindt O. J Appl Polym Sci 2000;76:495–508.
[6] Bermejo JS, Ugarte CM. Macromol Theory Simul 2009;18:259–67.
[7] Bermejo JS, Ugarte CM. Macromol Theory Simul 2009;18:317–27.
[8] Morel E, Bellenger V, Bocquet M, Verdu J. J Mater Sci 1989;24:69–75.
[9] Ellis B, Found MS, Bell JR. J Appl Polym Sci 2001;82:1265–76.
[10] Marks MJ, Snelgrove RV. Appl Mater Interface 2009;1:921–6.
[11] Pascault JP, Sautereau H, Verdu J, Williams RJJ. Thermosetting polymers. New York: Marcel Dekker Inc; 2002.
[12] Rottler J, Robbins MO. Phys Rev E 2001;64:051801.
[13] Lyulin AV, Vorselaars B, Mazo MA, Balabaev NK, Michels MAJ. Europhys Lett 2005;71:618–24.
[14] MacNeill D, Rottler J. Phys Rev E 2010;81:011804.
[15] Li CY, Strachan A. Polymer 2010;51:6058–70.
[16] Varshney V, Patnaik SS, Roy AK, Farmer BL. Macromolecules 2008;41:6837–42.
[17] Mayo SL, Olafson BD, Goddard III WA. J Phys Chem 1990;94:8897–909.
[18] LAMMPS (Large-scale Atomic/Molecular Massively Parallel Simulator), Open source code, http://www.cs.sandia.gov/~sjplimp/lammps.html.
[19] Li CY, Strachan A. Molecular dynamics simulations and experimental studies on glassy and rubbery thermomechanical properties of thermoset EPON825/33DDS. (To be published).
[20] Jang SS, Goddard WA. J Chem Phys C 2007;111:2759–69.
[21] See the online supplementary material.
[22] Sun L, Warren GL, O'Reilly JY, Everett WN, Lee SM, Davis D, et al. Carbon 2008;46:320–8.
[23] Tao K, Yang SY, Grunlan JC, Kim Y-S, Dang B, Deng YJ, et al. J Appl Polym Sci 2006;102:5248–54.
[24] Williams ML, Landel RF, Ferry JD. J Am Chem Soc 1955;77:3701–7.
[25] Ferry JD. Viscoelastic properties of polymers. New York: John Wiley & Sons Inc.; 1980.
[26] Nielsen LE. J Macromol Sci Revs Macromol Chem 1969;C3:69.
[27] Pascault JP, Williams RJJ. J Polym Sci B 1990;28:85–95.
[28] Zhou YX, Pervin F, Lewis L, Jeelani S. Mater Sci Eng A 2007;452–453:657–64.
[29] Tack, J.L., Thermodynamic and mechanical properties of EPON 862 with curing agent DETDA by molecular simulation. Master's thesis, Texas A&M University, 2006.
[30] Buckley CP, Harding J, Hou JP, Ruiz C, Trojanowski A. J Mech Phys Solids 2001;49:1517–38.
[31] Lyulin AV, Michels MAJ. Phys Rev Lett 2007;99:085504.
[32] Lesser AJ, Kody RS. J Polym. Sci Part B: Polym Phys 1997;35:1611–9.
[33] Lesser AJ, Calzia KJ. J Polym. Sci Part B Polym Phys 2004;42:2050–6.
[34] Caruthers J, Adolf DB, Chambers RS, Shrikhande P. Polymer 2004;45:4577–97.